OPEN ACCESS

Weak value measurement with an incoherent measuring device

To cite this article: Young-Wook Cho *et al* 2010 *New J. Phys.* **12** 023036

View the article online for updates and enhancements.

Related content

Recent citations

New Journal of Physics

Weak value measurement with an incoherent measuring device

Young-Wook Cho[1]**, Hyang-Tag Lim, Young-Sik Ra and Yoon-Ho Kim**[1]

Department of Physics, Pohang University of Science and Technology (POSTECH), Pohang 790-784, Korea
E-mail: choyoungwook81@gmail.com and yoonho72@gmail.com

Abstract. In the Aharonov–Albert–Vaidman (AAV) weak measurement, it is assumed that the measuring device or the pointer is in a quantum mechanical pure state. In reality, however, it is often not the case. In this paper, we generalize the AAV weak measurement scheme to include more generalized situations in which the measuring device is in a mixed state. We also report an optical implementation of the weak value measurement in which the incoherent pointer is realized with the pseudo-thermal light. The theoretical and experimental results show that the measuring device under the influence of partial decoherence could still be used for amplified detection of minute physical changes and is applicable for implementing the weak value measurement for massive particles.

[1] Authors to whom any correspondence should be addressed.

IOP Institute of Physics Φ DEUTSCHE PHYSIKALISCHE GESELLSCHAFT

Contents

1. Introduction

In von Neumann's measurement model, the process of measurement is considered as an interaction between the quantum system to be measured and the measuring device (or the pointer) with the assumption that the pointer state is initially prepared with a small uncertainty [1]. The projection postulate of the quantum theory, justified by von Neumann's measurement model, states that the outcome of a measurement on a quantum system must be one of the eigenvalues of the system's observable. The weak value introduced by Aharonov, Albert and Vaidman, however, is quite peculiar in that the measurement outcomes of the weak value may lie well outside the normal range of the eigenvalues of the measurement operator [2]. The weak value measurement, nevertheless, does not violate standard quantum theory and the effect is understood to be due to quantum interference of complex amplitudes [3].

The Aharonov–Albert–Vaidman (AAV) weak value measurement is accomplished in two steps: the weak measurement followed by postselection. The postselection step is the standard projection measurement (i.e. strong measurement) but, for the weak measurement, the measuring device or the pointer is assumed to be in a quantum mechanical pure state [2, 3]. In the case of quantum mechanical particles with mass whose center-of-mass coordinates are considered as the pointer for the measuring device, it becomes extremely difficult to achieve the measuring device in a pure state because the coupling to the environment causes decoherence of the pointer state as demonstrated, for example, in decoherence of matter waves [4]–[6] and degradation of an atom laser beam [7]. It is thus not surprising that the AAV weak value measurement to date has been implemented only with light whose spatial or temporal coherence can be used to represent the pointer in a pure state [8]–[16]. One is then led to a natural question whether the AAV weak value measurement must be performed with a pure pointer state and, recently, it has been shown theoretically that the AAV weak value measurement can indeed be performed with an arbitrary pointer state [17].

In this paper, we generalize the original AAV weak value measurement to include a more generalized situation in which the measuring device is in a mixed state. In particular, we consider the AAV weak value effect for a Gaussian-shaped pointer state whose degree of coherence can be varied continuously. (Our work therefore can be viewed as an experimentally relevant specific case of the general result reported in [17].) We then report an optical implementation of

the weak value measurement in which the Gaussian-shaped pointer with variable decoherence is realized with the pseudo-thermal light. The theoretical and experimental results suggest that the measuring device under the influence of partial decoherence, i.e. the pointer state with partial coherence (or a density matrix with nonzero off-diagonal elements), could still be used for amplified detection of weak effects.

2. Theory

2.1. Weak value measurement with a coherent measuring device

We start with a brief description of the AAV weak value measurement [2, 3]. The impulse interaction Hamiltonian between the pointer and the system, whose observable $\hat{A}$ is to be measured, is given in general as

$$\hat{H} = \delta(t - t_0)\hat{p}\hat{A}, \tag{1}$$

where $\hat{p}$ represents the momentum operator for the measuring device (with the conjugate position operator $\hat{q}$) and t_0 is the time of measurement (i.e. interaction). In the AAV weak value measurement [2, 3], the system is prepared in a pure state $|\psi_{\text{in}}\rangle$. The initial state of the pointer (i.e. the measuring device) is also assumed to be in a pure state (q-representation) as

$$|\phi_{\text{in}}\rangle = \left(\frac{2}{\pi w_0^2}\right)^{1/4} \int dq \, \exp(-q^2/w_0^2)|q\rangle, \tag{2}$$

where w_0 quantifies the pointer spread. With the inner product $\langle p|q\rangle = \exp(-ipq/\hbar)/\sqrt{2\pi\hbar}$, the pointer state in equation (2) can be rewritten in p-representation as

$$|\phi_{\text{in}}\rangle = \left(\frac{w_0^2}{2\pi\hbar^2}\right)^{1/4} \int dp \, \exp(-w_0^2 p^2/4\hbar^2)|p\rangle. \tag{3}$$

After the interaction in equation (1), the quantum state of both the system and the pointer evolves into

$$\exp(-i\hat{p}\hat{A}/\hbar)|\psi_{\text{in}}\rangle|\phi_{\text{in}}\rangle. \tag{4}$$

If we now make a projection measurement on the system in the $|\psi_f\rangle$ basis (i.e. postselection of the system having the quantum state $|\psi_f\rangle$), the pointer state is found to be

$$\langle\psi_f|\exp\left(-i\hat{p}\hat{A}/\hbar\right)|\psi_{\text{in}}\rangle|\phi_{\text{in}}\rangle \simeq (\langle\psi_f|\psi_{\text{in}}\rangle - i\hat{p}\langle\psi_f|\hat{A}|\psi_{\text{in}}\rangle/\hbar + \cdots)|\phi_{\text{in}}\rangle$$

$$\simeq N\langle\psi_f|\psi_{\text{in}}\rangle \int dp \, \exp\left(-\frac{w_0^2 p^2 + 4iA_{\text{w}}p}{4\hbar^2}\right)|p\rangle, \tag{5}$$

where $N \equiv (w_0^2/2\pi\hbar^2)^{1/4}$ and A_{w} is the weak value defined as [2, 3]

$$A_{\text{w}} \equiv \frac{\langle\psi_f|\hat{A}|\psi_{\text{in}}\rangle}{\langle\psi_f|\psi_{\text{in}}\rangle}. \tag{6}$$

Note that equation (5) has been derived with the assumption

$$\max_{n=2,3..} \left| \frac{\langle\psi_f|\hat{A}^n|\psi_{\text{in}}\rangle(\Delta p/\hbar)^n}{\langle\psi_f|\psi_{\text{in}}\rangle} \right| \ll |\Delta p A_{\text{w}}/\hbar| \ll 1, \tag{7}$$

where Δp is the spread of the pointer state in the p-represenation.

Using equations (2) and (3), we can re-write equation (5) as

$$\left(\frac{2}{\pi w_0^2}\right)^{1/4} \langle\psi_f|\psi_{\text{in}}\rangle \int dq \, \exp\left[-\frac{(q-A_{\text{w}})^2}{w_0^2}\right] |q\rangle. \tag{8}$$

The essence of the weak value measurement is illustrated in equation (8): the pointer displays, as an outcome of the measurement, the weak value A_{w}, which may be much larger than any eigenvalues of $\hat{A}$ if $|\psi_{\text{in}}\rangle$ and $|\psi_f\rangle$ are nearly orthogonal to each other.

Although approximations were used to derive equation (8), it is in fact possible to calculate the effect of the AAV weak value measurement without any approximation. By expanding $|\psi_{\text{in}}\rangle$ and $|\psi_f\rangle$ in the eigenbasis of $\hat{A}$ as $|\psi_{\text{in}}\rangle = \sum_k \alpha_k |a_k\rangle$ and $|\psi_f\rangle = \sum_l \beta_l |a_l\rangle$, the probability distribution $P_\psi(q)$ of the pointer q is explicitly calculated to be

$$
\begin{aligned}
P_\psi(q) &= \left| \langle q| \langle\psi_f|\hat{U}|\psi_{\text{in}}\rangle|\phi_{\text{in}}\rangle \right|^2 \\
&= \left| \left(\frac{2}{\pi w_0^2}\right)^{1/4} \sum_k \alpha_k \beta_k^* \exp\left[-\frac{(q-a_k)^2}{w_0^2}\right] \right|^2 \\
&= \sqrt{\frac{2}{\pi w_0^2}} \sum_{k,j} \alpha_k \beta_k^* \alpha_j^* \beta_j \exp\left[-\frac{(q-a_k)^2 + (q-a_j)^2}{w_0^2}\right],
\end{aligned}
\tag{9}
$$

where $\hat{U} = \exp(-i\hat{p}\hat{A}/\hbar)$, a_j and a_k are the eigenvalues of $\hat{A}$, and we have used the orthonormality condition $\langle a_l|a_k\rangle = \delta_{l,k}$. Note that, in the weak value measurement limit shown in equation (7), $P_\psi(q)$ in equation (9) approximates to a single Gaussian peaked at the weak value A_{w}.

2.2. Weak value measurement with an incoherent measuring device

So far, we have considered the case in which the measuring device is in a pure state, i.e. the pointer spread is completely coherent as shown in equation (2). Let us now generalize the problem by considering that the measuring device (having the same pointer spread w_0) is no longer in a pure state, but rather in a mixed state with some partial coherence quantified with w_{c}. The pointer state is then expressed as a density matrix

$$\rho_\phi = \frac{\sqrt{2}}{\pi w_0 w_{\text{c}}} \int dq_0 \, dq' \, dq'' \exp\left[-\frac{q_0^2}{w_0^2}\right] \exp\left[-\frac{(q'-q_0)^2}{w_{\text{c}}^2}\right] \exp\left[-\frac{(q''-q_0)^2}{w_{\text{c}}^2}\right] |q'\rangle\langle q''|, \tag{10}$$

and the initial system-pointer quantum state is described as

$$|\psi_{\text{in}}\rangle \rho_\phi \langle\psi_{\text{in}}|. \tag{11}$$

After the weak measurement, the initial system-pointer density matrix $|\psi_{\text{in}}\rangle \rho_\phi \langle\psi_{\text{in}}|$ is evolved due to the interaction Hamiltonian in equation (1) into

$$\hat{U}|\psi_{\text{in}}\rangle \rho_\phi \langle\psi_{\text{in}}|\hat{U}^\dagger. \tag{12}$$

Making a projection measurement on the system in the $|\psi_f\rangle$ basis (i.e. postselecting the system having the state $|\psi_f\rangle$), the pointer state is found to be

$$
\begin{aligned}
\rho_f &= \langle\psi_f|\hat{U}|\psi_{\text{in}}\rangle \rho_\phi \langle\psi_{\text{in}}|\hat{U}^\dagger|\psi_f\rangle \\
&= \sum_{k,j,l,m} \beta_l^* \alpha_k \alpha_j^* \beta_m \langle a_l|\hat{U}|a_k\rangle \rho_\phi \langle a_j|\hat{U}^\dagger|a_m\rangle.
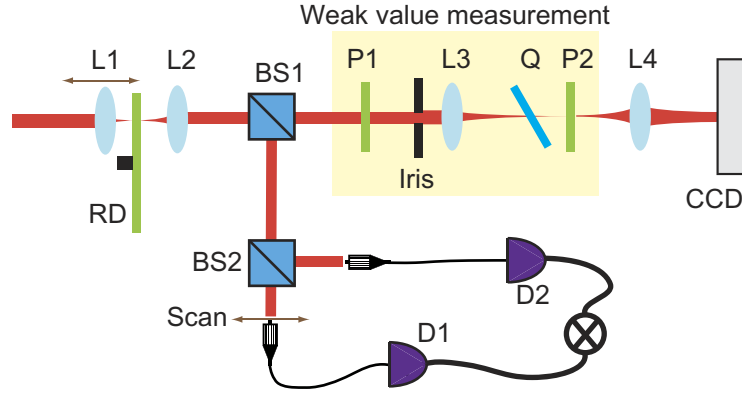\end{aligned}
\tag{13}
$$

Figure 1. Schematic of the experiment. The incoherent pointer state is realized with a pseudo-thermal light source whose transverse spatial coherence can be varied. An He–Ne laser beam is focused on an RD with a movable lens L1 and the scattered light is collimated with another lens L2. BS1 and BS2 are 50/50 beam splitters. The transverse spatial coherence of the beam is measured with detectors D1 and D2 and is used for determining γ, the degree of partial coherence of the pointer state. P1 and P2 are polarizers for state preparation and postselection, respectively. The weak measurement occurs at the tilted quartz plate Q.

The probability distribution for the pointer $P_\rho(q)$ is then calculated as

$$
\begin{aligned}
P_\rho(q) &= \langle q|\rho_f|q\rangle \\
&= \frac{\sqrt{2}}{\pi w_0 w_c} \sum_{k,j} \alpha_k \beta_k^* \alpha_j^* \beta_j \int dq_0 \exp\left[-\frac{q_0^2}{w_0^2} - \frac{(q-a_k-q_0)^2}{w_c^2} - \frac{(q-a_j-q_0)^2}{w_c^2}\right] \\
&= \sqrt{\frac{2}{\pi(2w_0^2+w_c^2)}} \sum_{k,j} \alpha_k \beta_k^* \alpha_j^* \beta_j \exp\left[w_0^{-2}\left(-\frac{(q-a_k)^2}{\gamma^2} - \frac{(q-a_j)^2}{\gamma^2} + \frac{(2q-a_k-a_j)^2}{\gamma^4+2\gamma^2}\right)\right],
\end{aligned}
$$

(14)

where we have used the orthonormality conditions $\langle a_l|a_k\rangle = \delta_{l,k}$ and $\langle a_j|a_m\rangle = \delta_{j,m}$. Note that the degree of partial coherence is defined as $\gamma \equiv w_c/w_0$.

Equation (14) shows that the weak value effect should still be observable even though the measuring device (i.e. the pointer) is in a mixed state whose degree of partial coherence is quantified with γ. Note that the pointer is effectively in a pure state in the limit $\gamma \gg 1$ and, in this limit, equation (14) approximates to equation (9).

3. Experiment

The weak value measurement setup that incorporates the pointer in a mixed state is schematically shown in figure 1. The system state is the polarization state of the photon (analogous to a spin-1/2 particle) and is assumed to be in a pure state. The transverse position of the photon corresponds to the pointer (i.e. the measuring device) for measuring the system state [3, 8].

The incoherent pointer state is realized with the pseudo-thermal light source based on scattering of a focused laser beam (an He–Ne laser operating at 632.8 nm) at a rotating ground disc (RD) [18]. Because the scattered light at RD is spatially incoherent in the transverse direction of the beam, the pointer state can be expressed in the form of equation (10). The focusing (L1) and collimating (L2) lenses have 30 and 75 mm focal lengths, respectively. By moving L1 longitudinally, thereby changing the beam size on the RD, the degree of transverse spatial coherence of the collimated beam can be varied. Therefore, we can easily adjust the degree of partial coherence γ of the pointer state in equation (14) by simply moving the focusing lens L1. The collimated beam is then split into two by a beam splitter (BS1); one beam is for the weak value measurement and the other is for characterizing the pointer state.

For the weak value measurement, the photon is prepared in a definite polarization state with polarizer P1. An iris placed after P1 defines the e^{-2} beam waist radius $w'_0 = 0.697$ mm. The lens L3 ($f = 100$ mm) then focuses the beam so that the beam waist is $w_0 = \lambda f/(\pi w'_0) = 28.9\,\mu$m at the focus. The weak measurement on the system (i.e. the polarization state of the photon) is then implemented with a 0.5 mm thick quartz plate Q with its optic axis oriented vertically. The quartz plate Q causes a small polarization-dependent displacement between the two orthogonal polarization components due to the birefringence. The measurement operator $\hat{A}$ that corresponds to this experimental situation can be expressed as

$$\hat{A} = a|V\rangle\langle V|, \tag{15}$$

where a is the expected spatial displacement given, in this case, as $a = 1.316\,\mu$m. Clearly, the expected displacement is much smaller than the beam width w_0 and, therefore, the quartz plate Q acts as the weak measurement operator on the system [3, 8]. In order to ensure that the incoming polarization of the photon is not changed by Q, i.e. the net phase difference of 2π between the vertical and horizontal polarizations of the photon, Q was tilted (about the optic axis) to $43.5°$.

After the weak measurement by quartz plate Q, the postselection measurement (on polarization) is implemented by the polarizer P2 placed at the focus of L3. Finally, an imaging lens L4 ($f = 50$ mm) and a CCD camera are used to measure the transverse spatial profile of the photon at the P2 location.

4. Results and analysis

4.1. Characterizing the incoherent measuring device (pointer state)

As mentioned earlier, we can vary the transverse spatial coherence of the collimated beam by changing the beam size on the RD and the degree of transverse spatial coherence is directly related to the degree of partial coherence γ in equation (14). Therefore, the first step in experimentally demonstrating the weak value measurement with an incoherent measuring device is to properly and accurately characterize the transverse spatial coherence of the collimated beam.

In the experiment, the light scattered at the RD is collimated with L2. Beam splitter BS2 then splits the collimated beam: the transmitted beam is used for the weak value measurement and the reflected beam is used for measuring the transverse spatial coherence of the pointer, see figure 1. The degree of transverse spatial coherence of the beam is measured with a Hanbury–Brown–Twiss-type interferometer, consisting of a 50/50 beam splitter (BS2) and two detectors D1 and D2. The detectors D1 and D2 are multi-mode fiber coupled so that the effective diameter of the detectors is $62.5\,\mu$m, the core diameter of the fiber. The fiber connected to D1 can be scanned and the photocurrents from the detectors D1 and D2 are digitized and stored on
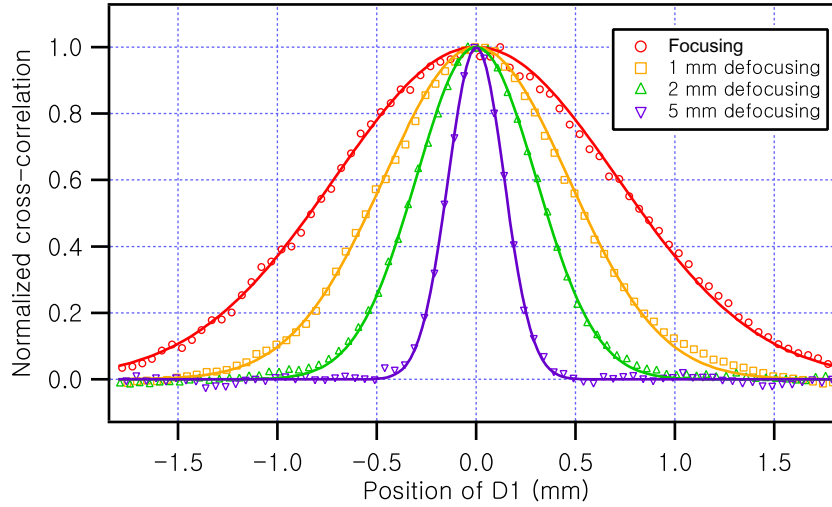
Figure 2. The normalized cross-correlation, $C(x)$, as a function of D1 position, x, shows the degree of transverse spatial coherence of the collimated beam. The measured e^{-2} widths w_c' are 1.42, 0.93, 0.60 and 0.28 mm. The w_c values for the weak value measurement can be calculated from w_c' and they are 59.0, 38.5, 25.0 and 11.7 μm, respectively. The degree of partial coherence γ can then be calculated using the relation $\gamma = w_c/w_0$. The pointer spread w_0 is kept constant at 28.9 μm. See text for details.

a computer. The cross-correlation between the two split modes (of BS2) is then calculated using the ac components of the digitized photocurrents, $\Delta I(t)$, using the relation

$$C(x) = \frac{\langle \Delta I_1(x,t) \Delta I_2(t) \rangle_t}{\sqrt{\langle (\Delta I_1(x,t))^2 \rangle_t} \sqrt{\langle (\Delta I_2(t))^2 \rangle_t}} = g^{(2)}(x) - 1, \tag{16}$$

where subscripts 1 and 2 refer to detectors D1 and D2, respectively, and $\langle \ldots \rangle_t$ represents time averaging. Note that $C(x)$ is a direct measurement of the deviation from unity for the normalized second-order correlation function $g^{(2)}(x)$ [19] .

The experimental results are shown in figure 2. The cross-correlation measurements show that defocusing of L1 causes reduction of the transverse spatial coherence of the collimated beam. The measured e^{-2} widths w_c' are 1.42, 0.93, 0.60 and 0.28 mm, depending on the L1 position. Because the weak value measurement setup uses lens L3 ($f = 100$ mm) to focus the beam, see figure 1, the measured value w_c' should be converted to the value relevant in the weak value measurement setup using the relation $w_c = w_c' w_0/w_0'$. As discussed in the previous section, $w_0' = 0.698$ mm and $w_0 = \lambda f/(\pi w_0') = 28.9$ μm. The degree of partial coherence γ in equation (14) is then calculated using the relation $\gamma = w_c/w_0$. The γ values are 2.04 (focusing), 1.33 (1 mm defocusing), 0.865 (2 mm defocusing) and 0.404 (5 mm defocusing).

4.2. Weak value measurement with an incoherent measuring device

Since the degree of partial coherence γ is determined for the measuring device (i.e. the pointer state), we now can proceed to test weak value measurement with an incoherent measuring device. We start by re-writing the general result in equation (14) using experimentally relevant parameters.
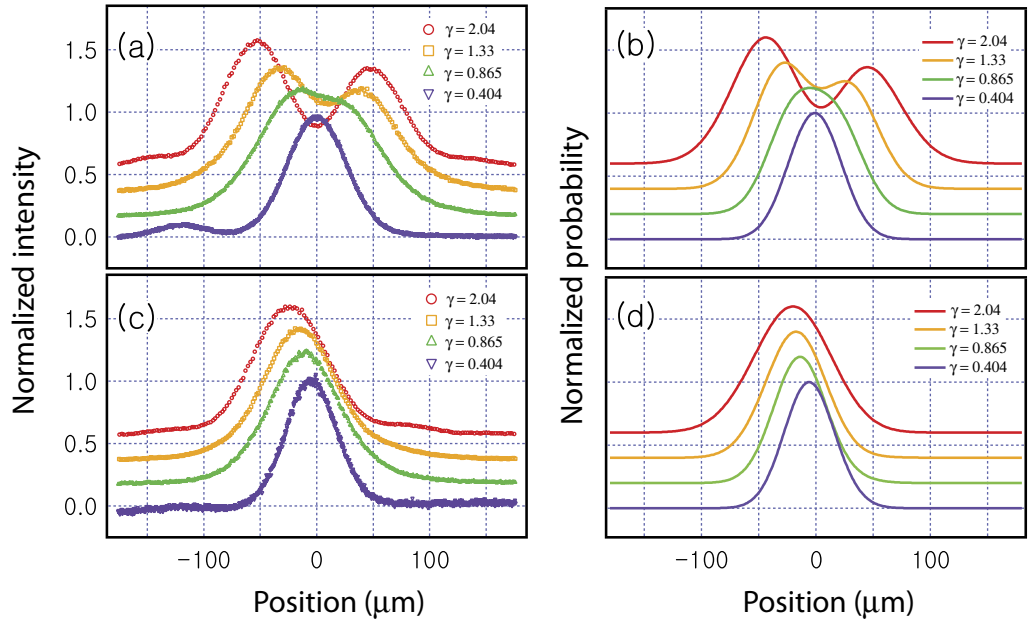
Figure 3. Weak value measurement with an incoherent measuring device. (a) and (c) are experimental data and (b) and (d) are corresponding theoretical results plotted using equation (17). For (a) and (b), $\epsilon = 1.00 \times 10^{-3}$ rad. For (c) and (d), $\epsilon = 2.79 \times 10^{-2}$ rad. All plots are normalized to unity and vertically shifted for clarity. For (b), the peak probabilities are 9.98×10^{-7}, 2.74×10^{-6}, 8.47×10^{-6} and 5.52×10^{-5} for γ values of 2.04, 1.33, 0.865 and 0.404, respectively. For (d), the peak probabilities are 1.08×10^{-5}, 1.63×10^{-5}, 2.52×10^{-5} and 7.18×10^{-5} for γ values of 2.04, 1.33, 0.865 and 0.404, respectively.

In the experiment, the initial and final polarization states of the photon are assumed linear (P1 and P2 are linear polarizers) so that $|\psi_{\text{in}}\rangle = \cos\alpha|H\rangle + \sin\alpha|V\rangle$ and $|\psi_f\rangle = \cos\beta|H\rangle + \sin\beta|V\rangle$. Since $|\psi_{\text{in}}\rangle$ and $|\psi_f\rangle$ should be almost orthogonal to observe the weak value effect, P1 and P2 angles are set at $\alpha = \pi/4$ and $\beta = -\pi/4 + \epsilon$, respectively. Also, the eigenvalues of the observable, corresponding to the expected beam shift for each polarization state, are $a_H = -a$ and $a_V = 0$. Under these conditions, equation (14) can be re-written as

$$P_\rho(q) \propto \cos^2\beta \exp\left[w_0^{-2}\left(-\frac{2(a+q)^2}{\gamma^2} + \frac{4(a+q)^2}{\gamma^4 + 2\gamma^2}\right)\right] + \sin^2\beta \exp\left[w_0^{-2}\left(-\frac{2q^2}{\gamma^2}\frac{4q^2}{\gamma^4 + 2\gamma^2}\right)\right]$$

$$+ \sin 2\beta \exp\left[w_0^{-2}\left(-\frac{a^2 + 2aq + 2q^2}{\gamma^2} + \frac{(a+2q)^2}{\gamma^4 + 2\gamma^2}\right)\right]. \tag{17}$$

We have performed the weak value measurement with the incoherent pointer for several values of γ, which characterizes the degree of partial coherence of the pointer (i.e. the measuring device), and for two values of ϵ, which determines the $\langle\psi_f|\psi_{\text{in}}\rangle$ value. Note that, since the weak value A_w does not make sense if $\langle\psi_f|\psi_{\text{in}}\rangle = 0$, ϵ should not be zero. (If $\langle\psi_f|\psi_{\text{in}}\rangle = 0$, the weak value is not defined by the definition of equation (6), and the assumption of equation (7) cannot be satisfied.) To obtain a large weak value A_w, however, ϵ should be close to zero.

The experimental results and corresponding theoretical results are shown in figure 3. In experiment, the peak position of the measured transverse spatial profile of the beam on the CCD
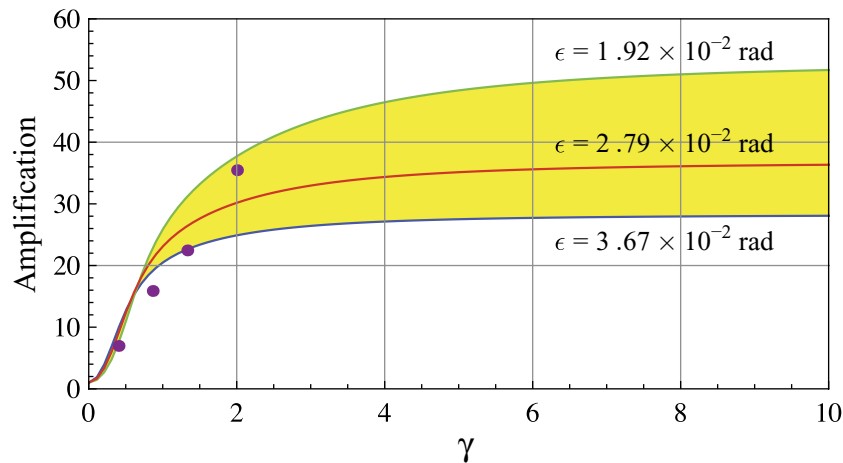
Figure 4. Weak value amplification as a function of γ. Experimental data points are from figure 3(c) for $\epsilon = 2.79 \times 10^{-2}$ rad. For each data point, the error bars are smaller than the solid circle. The solid lines are due to the theoretical result in equation (17). The upper and lower solid lines are for the weak value amplification calculated for $\epsilon = 1.92 \times 10^{-2}$ and 3.67×10^{-2} rad, respectively. These ϵ values correspond to relative angle setting errors of $\pm 0.5°$ between polarizers P1 and P2 (The angle setting error of $\pm 0.5°$ comes from the fact that our rotation mounts were graded in $2°$ increments.).

represents the weak value A_w. The experimental results show that the weak value A_w, which is larger than the eigenvalue of the operator $a_\mathrm{H} = -a = -1.316\,\mu$m, is observable even with the pointer (measuring device) in a mixed state if the pointer has some degree of partial coherence, i.e. nonzero off-diagonal elements of the density matrix representing the pointer state. Note also that the larger the degree of partial coherence γ, the larger the resulting weak value A_w.

The experimental data also show that if ϵ is too close to zero ($\epsilon = 1.00 \times 10^{-3}$ rad), the weak value is not well defined, see figure 3(a). The spatial profile shows two peaks when the γ is large enough, but it reduces to a single Gaussian peak centered nearly at zero when γ is much smaller than 1. This clearly is due to the lack of quantum interference.

The weak value effect is more clearly visible for a slightly larger value of ϵ, $\epsilon = 2.7 \times 10^{-2}$ rad. As shown in figure 3(c), the weak value effect is reduced gradually as γ gets smaller. Even for a rather small value $\gamma = 0.404$ (an incoherent pointer with small partial coherence), a rather large weak value $A_\mathrm{w} = -4.58 \pm 0.0742\,\mu$m is observed. The experimental results, figures 3(a) and (c), are in good agreement with the theoretical plots, figures 3(b) and (d), calculated using equation (17).

It is interesting to note that, in figure 3, smaller uncertainties (widths of the peaks) are obtained with smaller values of γ. It should also be noted that the smaller the value of γ, the larger the peak probability (see the caption of figure 3). This implies that the weak value effect is strongly postselective: to obtain a larger weak value amplification effect, the probability of the event must be sacrificed.

Finally, the weak value effect as a function of γ is summarized in figure 4, which shows that the amplification (defined as the ratio between the peak position of the spatial profile and the expectation value of the observable $\hat{A}$, i.e. $\langle\psi_\mathrm{in}|\hat{A}|\psi_\mathrm{in}\rangle = -a/2 = -0.658\,\mu$m) depends heavily on γ and ϵ. For $\gamma \gg 1$, the pointer state becomes effectively pure so that the amplification

IOP Institute of Physics Φ DEUTSCHE PHYSIKALISCHE GESELLSCHAFT

factor is bounded to a specific value. In the intermediate range of γ, the amplification factor increases as γ gets larger. We would like to point out that the weak value amplification can still be observed even for $\gamma < 1$. Of course, if the pointer is completely incoherent (i.e. $\gamma = 0$), no weak value effect can occur (i.e. no amplification).

5. Conclusion

We have generalized the AAV weak value effect to include the situations in which the measuring device (the pointer) is in a mixed state and have demonstrated the generalized weak value effect in an optical experiment in which the pointer in a mixed state is realized with the pseudo-thermal light source of a varying degree of partial spatial coherence. We have also introduced an experimentally measurable quantity that effectively quantifies the partial coherence of the pointer. Our results show that the pointer state, no longer in a pure state but in a mixed state (with some partial coherence) can still exhibit the weak value effect and thus may be used for amplified detection of very small physical changes. The result reported in this paper should be directly applicable to weak value measurement schemes involving a beam of massive particles whose pointer states (the transverse profile of the beam) cannot be expected to be in a pure state due to the decoherence-causing interactions, such as inter-particle collisions, strong coupling with the environment, etc.

Acknowledgments

References

[1] von Neumann J 1955 *Mathematical Foundations of Quantum Mechanics* (Princeton, NJ: Princeton University Press)
[2] Aharonov Y, Albert D Z and Vaidman L 1988 *Phys. Rev. Lett.* **60** 1351–4
[3] Duck I M, Stevenson P M and Sudarshan E C G 1989 *Phys. Rev.* D **40** 2112–7
[4] Kleckner M and Ron A 2001 *Phys. Rev.* A **63** 022110
[5] Arndt M, Nairz O, Vos-Andreae J, Keller C, der Zouw G V and Zeilinger A 1999 *Nature* **401** 680–2
[6] Hackermüller L, Hornberger K, Brezger B, Zeilinger A and Arndt M 2004 *Nature* **427** 711–4
[7] Riou J F, Guerin W, Le Coq Y, Fauquembergue M, Josse V, Bouyer P and Aspect A 2006 *Phys. Rev. Lett.* **96** 070404
[8] Ritchie N W M, Story J G and Hulet R G 1991 *Phys. Rev. Lett.* **66** 1107–10
[9] Resch K J, Lundeen J S and Steinberg A M 2004 *Phys. Lett.* A **324** 125–31
[10] Solli D R, McCormick C F and Chiao R Y 2004 *Phys. Rev. Lett.* **92** 043601
[11] Pryde G J, O'Brien J L, White A G, Ralph T C and Wiseman H M 2005 *Phys. Rev. Lett.* **94** 220405
[12] Ralph T C, Bartlett S D, OBrien J L, Pryde G J and Wiseman H M 2006 *Phys. Rev.* A **73** 012113
[13] Wang Q, Sun F-W, Zhang Y-S, Li J, Huang Y-F and Guo G-C 2006 *Phys. Rev.* A **73** 023814
[14] Hosten O and Kwiat P 2008 *Science* **319** 787–90
[15] Lundeen J S and Steinberg A M 2009 *Phys. Rev. Lett.* **102** 020404
[16] Dixon P B, Starling D J, Jordan A N and Howell J C 2009 *Phys. Rev. Lett.* **102** 173601
[17] Johansen L M 2004 *Phys. Rev. Lett.* **93** 120402
[18] Martienssen W and Spiller E 1964 *Am. J. Phys.* **32** 919–26
[19] Loudon R 2000 *The Quantum Theory of Light* (Oxford: Oxford University Press)